Spectral behavior of second harmonic signals from organic and non-organic materials in multiphoton microscopy

Tobias Ehmke, Andreas Knebl, Stephan Reiss, Isaak R. Fischinger, Theo G. Seiler, Oliver Stachs, and Alexander Heisterkamp

Citation: AIP Advances **5**, 084903 (2015); doi: 10.1063/1.4915134

View online: http://dx.doi.org/10.1063/1.4915134

View Table of Contents: http://aip.scitation.org/toc/adv/5/8

Published by the American Institute of Physics

Spectral behavior of second harmonic signals from organic and non-organic materials in multiphoton microscopy

Tobias Ehmke,[1,a] Andreas Knebl,[1] Stephan Reiss,[2,3] Isaak R. Fischinger,[4] Theo G. Seiler,[4] Oliver Stachs,[3] and Alexander Heisterkamp[5]
[1]*Institute of Applied Optics, Friedrich-Schiller-University Jena, Froebelstieg 1, 07743 Jena, Germany*
[2]*Institute for Physics, Semiconductor Optics Group, University of Rostock, 18055 Rostock, Germany*
[3]*Department of Ophthalmology, University of Rostock, 18057 Rostock, Germany*
[4]*Institut fuer Refraktive und Ophthalmo-Chirurgie (IROC), Stockerstrasse 37, 8002 Zuerich, Switzerland*
[5]*Institute of Quantum Optics, University of Hanover, 30167 Hanover, Germany*

(Received 26 August 2014; accepted 9 January 2015; published online 12 March 2015)

Multimodal nonlinear microscopy allows imaging of highly ordered biological tissue due to spectral separation of nonlinear signals. This requires certain knowledge about the spectral distribution of the different nonlinear signals. In contrast to several publications we demonstrate a factor of $\frac{1}{2\sqrt{2}}$ relating the full width at half maximum of a gaussian laser pulse spectrum to the corresponding second harmonic pulse spectrum in the spatial domain by using a simple theoretical model. Experiments on monopotassium phosphate crystals (KDP-crystals) and on porcine corneal tissue support our theoretical predictions. Furthermore, no differences in spectral width were found for epi- and trans-detection of the second harmonic signal. Overall, these results may help to build an optimized multiphoton setup for spectral separation of nonlinear signals. [http://dx.doi.org/10.1063/1.4915134]

Multiphoton microscopy is a powerful tool for ex- and in-vivo imaging of biological tissue.[1–6] Image formation in multiphoton systems is based on signals with a nonlinear nature like two-photon fluorescence, second-harmonic generation (SHG) or third harmonic generation (THG).[7–10]

One advantage of this technique is the possibility to generate different nonlinear signals inside the sample which can be spectrally seperated.[11] This leads to high contrast imaging.

A spectral overlap in different detection channels results in a limited achievable contrast. To realize a proper spectral separation, the spectral distribution of each signal has to be known exactly. On the one hand, fluorescence signals have broad spectral characteristics which are not related to the spectral distribution of the exciting laser pulse. Internal molecular transitions play a dominant role in the process of fluorescence. Parametric processes (for example generation of higher harmonics), on the other hand, exhibit a spectral distribution strongly dependent on the spectral distribution of the fundamental pump beam.

SHG is a second order nonlinear parametric process often used for imaging collagen and other media with a non-centrosymmetric molecular structure.[11–13] Previous publications in the field of biophysics reported the relationship between the spectral bandwidth of the second harmonic and the pump pulse.[14–16] Campagnola reported a narrowing factor of $1/\sqrt{2} = 0.707$ of the second harmonic frequency bandwidth compared to the fundamental pump pulse.[14] This is equal to a scaling factor of $1/(4\sqrt{2}) = 0.177$ in terms of wavelength bandwidth. In contrast, Zipfel *et al.*[15] and Mohler *et al.*[16] reported a factor of $1/\sqrt{2}$ between the bandwidth of the fundamental and the second harmonic in terms

[a]Electronic mail: t.ehmke@lzh.de

of wavelength. In contrast to these previous publications, we show a narrowing factor of $\frac{1}{2\sqrt{2}}$ between the spectral bandwidth of the fundamental laser pulse and the second harmonic pulse in the spatial domain. A simple analytical calculation for gaussian laser pulses yields this factor. Experiments on monopotassium phosphate crystals (KDP-crystals) and porcine cornea (biological tissue) support the result of this calculation.

The intensity distribution of a gaussian shaped pulse can be written as shown in Eq. (1):[17]

$$I(t) = I_0 \exp\left[-4\ln(2)\left(\frac{t}{\Delta\tau_{\text{fund}}}\right)^2\right] \tag{1}$$

I_0 stands for the peak intensity, t for the time and $\Delta\tau_{\text{fund}}$ for the full width at half maximum (FWHM) in the time domain of the gaussian fundamental laser pulse. Since the n-th harmonic signal intensity is proportional to I^n_{fund} the condition for calculating the FWHM of the n-th harmonic signal pulse is given by Eq. (2):

$$\left(\frac{1}{2}\right)^{\frac{1}{n}} = \exp\left[-4\ln(2)\left(\frac{t}{\Delta\tau_{\text{fund}}}\right)^2\right] \tag{2}$$

Solving Eq. 2 for t results in Eq. (3):

$$\frac{1}{4n} = \left(\frac{t}{\Delta\tau_{\text{fund}}}\right)^2 \Leftrightarrow t = \pm\frac{1}{2\sqrt{n}}\Delta\tau_{\text{fund}} \tag{3}$$

Based on the resulting t in Eq. (3), the FWHM Δt_n for the n-th harmonic signal pulse in the time domain can be expressed by Eq. (4):

$$\Delta t_n = \frac{1}{\sqrt{n}}\Delta\tau_{\text{fund}} \tag{4}$$

The pulse duration of a laser pulse is directly connected to its spectral distribution via the time-bandwidth product $\Delta\tau\Delta\nu \geq C$.[17] $\Delta\nu$ stands for the FWHM in the frequency domain and C is a constant depending on the pulse shape. For gaussian pulses commonly used for multiphoton microscopy $C = 0.4413$.[17] Assuming a constant time-bandwidth product for laser pulses and generated higher harmonic pulses leads to Eq. (5):

$$\Delta t_n \Delta\nu_n = \Delta\tau_{\text{fund}}\Delta\nu_{\text{fund}}. \tag{5}$$

Using Eq. (4) in Eq. (5) leads to an expression connecting the FWHM of the n-th harmonic signal pulse ($\Delta\nu_n$) with the FWHM of the fundamental laser pulse ($\Delta\nu_{\text{fund}}$) in the frequency domain:

$$\Delta\nu_n = \sqrt{n}\cdot\Delta\nu_{\text{fund}}. \tag{6}$$

The link between the frequency domain and the spatial domain is given in general by $\Delta\nu = \frac{c}{\lambda^2_{\text{central}}}\Delta\lambda$. Thus, Eq. (6) can be expressed in the spatial domain:

$$\frac{c}{\lambda^2_n}\Delta\lambda_n = \sqrt{n}\frac{c}{\lambda^2_{\text{fund}}}\Delta\lambda_{\text{fund}}. \tag{7}$$

Using the fact that $n\lambda_n = \lambda_{\text{fund}}$ finally leads to an expression relating $\Delta\lambda_n$ and $\Delta\lambda_{\text{fund}}$:

$$\Delta\lambda_n = \frac{1}{n\sqrt{n}}\Delta\lambda_{\text{fund}}. \tag{8}$$

In the special case of second harmonic generation ($n = 2$) a narrowing factor of $\frac{1}{2\sqrt{2}} = 0.354$ can be found.

In our setup a Chameleon Ultra II laser system (*Coherent Inc.*) with a pulse duration of nearly 170 fs at 798 nm central pulse wavelength (gaussian shape, measured at laser output) was used. Due to dispersion induced by several optics in the beam path, temporal broadening takes place. Thus, pulses with nearly 250 fs temporal width were measured in the sample plane. From Eq. (4), the

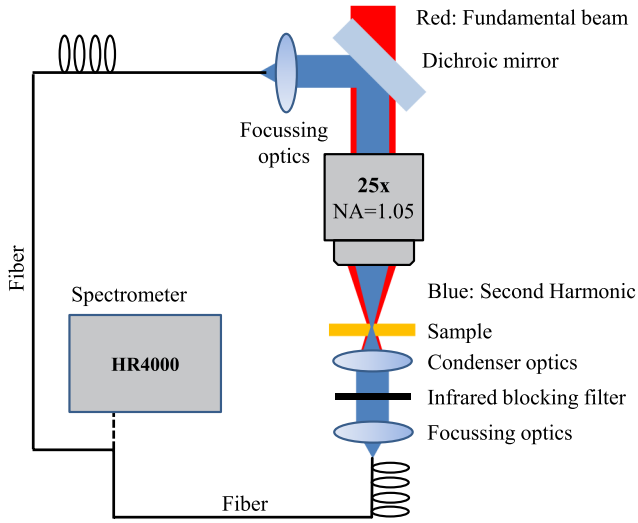

FIG. 1. Experimental setup: Two fibers were placed in the detection beam paths of the multiphoton microscope MPM200 in order to guide the second harmonic signal to a spectrometer. The setup allowed signal detection in epi- and trans-direction.

temporal width of a second harmonic pulse generated by the Chameleon Ultra II should then be $\frac{250}{\sqrt{2}}$ fs = 176.8 fs.

Assuming a FWHM of 5.5 nm at 798 nm central wavelength the FWHM of the second harmonic pulse generated at 399 nm central wavelength should therefore be $\frac{5.5}{2\sqrt{2}}$ nm = 1.94 nm.

To measure the spectral bandwidth of the second harmonic in epi- and trans-direction, two photomultipliers of our multiphoton microscope MPM200 (*Thorlabs*) were replaced with fibers and collection optics in order to guide the second harmonic signal to a HR4000 spectrometer (*Ocean Optics*). This setup allowed spectral detection in both epi- and trans-direction (Fig. 1).

In the first experiment the second harmonic signal was generated on 5 KDP crystals without known geometry. Phase matching was achieved by high-NA focussing (Objective lens: XLPL25XWMP (*Olympus*), NA = 1.05). During the spectral measurements, the scanning mirrors of the multiphoton microscope were fixed at their zero position. As expected, a narrowing of the spectral bandwidth of the fundamental laser pulses with a central wavelength at 798 nm in comparison with the second harmonic pulse spectra with a central wavelength at 399 nm can be observed for both mentioned detection modes (Fig. 2). The averaged FWHM for 5 measurements in forward direction is 2.3 ± 0.1 nm and in backward direction 2.2 ± 0.1 nm. This results in narrowing factors of 0.42 ± 0.03 for the forward direction and of 0.40 ± 0.03 for the backward direction.

In the second experiment, spectral measurements of the second harmonic generated in porcine corneas were performed. The stromal region of the cornea mostly consists of collagen fibers giving a strong second harmonic signal. Measurements were performed on native porcine corneas and crosslinked corneas while spectral detection was realized only in epi-direction. Crosslinking is a parasurgical treatment for keratoconus.[18] The crosslinking involves a one-time application of riboflavin solution to the eye that is activated by illumination with UV-A light.[18] The riboflavin causes additional chemical bonds to form across adjacent collagen strands in the stromal layer of the cornea, which recovers and preserves some of the cornea's mechanical strength. In each type of cornea, 7 different positions were used for the measurements. Similar to the experiments on KDP a strong narrowing of the FWHM can be observed when comparing the laser pulse with the second harmonic spectrum (Fig. 3). For 7 measurements the average FWHM is 2.2 ± 0.1 nm for non-crosslinked and crosslinked cornea. This results in a narrowing factor of 0.40 ± 0.03 for both types of cornea.

Depending on the domain (time domain, frequency domain and spatial domain), our theoretical calculation gives different factors relating the FWHM of a fundamental gaussian laser pulse to the n-th harmonic signal. This is summed up in Table I.

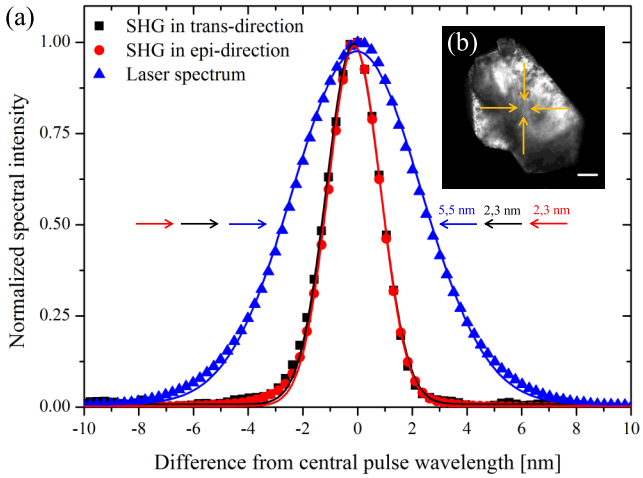

FIG. 2. Exemplary result of a spectral measurement: (a) Narrowing of the spectral width of the generated second harmonic signal in KDP in comparison to the laser pulse spectrum for epi- and trans-detection. Laser pulse: FWHM = 5.5 nm, central pulse wavelength = 798 nm; SHG: FWHM = 2.3 nm, central pulse wavelength = 399 nm. No distinct difference between the FWHM detected in different directions could be found. (b) Second harmonic image of the used KDP crystal when recording a scanned image after the spectral measurement (a dichroic mirror was inserted into the beam path and the second harmonic signal was detected with a photomultiplier tube). Arrows show the central image position where the second harmonic signal was generated for the spectral measurement. Scale bar: 50 μm.

The result for the spatial domain is of special interest. It differs from previous reports in the field of biophysics where for the second harmonic signal ($n = 2$), a narrowing of the spectral bandwidth with a factor of $1/(4\sqrt{2})$ or $1/\sqrt{2}$ was reported.[14–16]

The second harmonic spectrum measured on KDP shows a distinct narrowing in comparison with the spectrum of the laser pump beam (narrowing factors: 0.42 ± 0.03 (forward) and 0.40 ± 0.03 (backward)). Within the measurement accuracy of ±0.1 nm, no significant difference between the measured FWHM for forward and backward direction could be found.

Although our results are based on measurements with a high-NA objective lens (NA = 1.05, water immersion) they are in good agreement with experimental data published in several previous

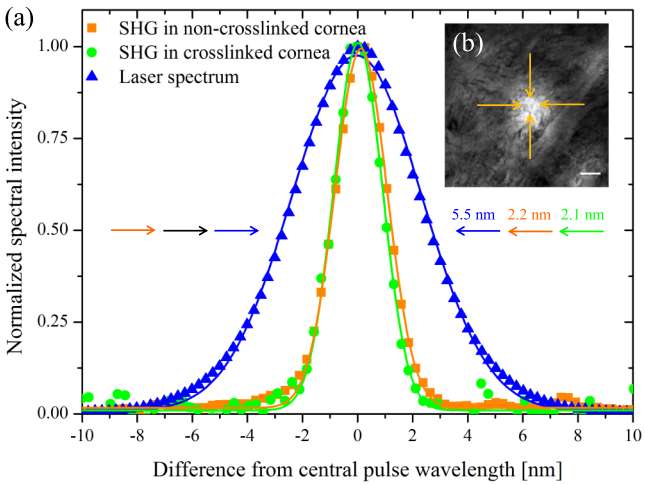

FIG. 3. Exemplary result of spectral measurements in epi-direction: (a) Narrowing of the spectral width of the generated second harmonic signal from cornea in comparison to the laser pulse spectrum. Central pulse wavelengths: 798 nm (laser pulse) and 399 nm (SHG). (b) Second harmonic image of the cornea when recording a scanned image after the spectral measurement. The arrows show the central image position where the second harmonic signal was generated for the spectral measurements. Scale bar: 50 μm.

TABLE I. Relation between the FWHM of a fundamental gaussian laser pulse and a resulting n-th harmonic signal in different domains.

Time domain	Frequency domain	Spatial domain
$\Delta t_n = \frac{1}{\sqrt{n}}\Delta\tau_{\text{fund}}$	$\Delta\nu_n = \Delta\nu_{\text{fund}}\sqrt{n}$	$\Delta\lambda_n = \frac{1}{n\sqrt{n}}\Delta\lambda_{\text{fund}}$

publications in the field of crystal optics.[19,20] Nevertheless, a spectral comparison of forward and backward detected second harmonic signals has not been done so far in the field of crystal optics. This comparison is of special interest for biomedical microscopy applications since in vivo imaging requires backward detection of nonlinear signals.

In several publications, the influence of the phase matching condition on the higher harmonic spectrum is discussed.[20,21] It is reported that different phase matching conditions can alter the shape of the spectrum.[20,21] Especially in the field of second harmonic microscopy, the appearance of backward generated second harmonic signals is predicted and the difference between phase matching conditions for forward and backward generated second harmonics is discussed by LaComb *et al.*[22] Considering the work of Zhang *et al.*[20] and Farrell *et al.*,[21] our experimental results imply nearly the same phase matching conditions for forward and backward generated second harmonic signals.

Since phase matching conditions in multiphoton microcopy are relaxed (high NA-focussing), no special attention was paid to phase matching in the theoretical calculation reported in this work.

Similar to KDP crystal samples, the results on porcine cornea (organic material) show a narrowing of the second harmonic signals in comparison to the fundamental laser pulse spectrum (narrowing factor: 0.4 ± 0.03 (non-crosslinked and crosslinked)). No significant difference between the FWHM of the spectral second harmonic signal in crosslinked and non-crosslinked corneas could be found for epi-detection. Thus, collagen crosslinking preserves the non-centrosymmetric molecular structure of collagen and has no effect on second harmonic generation.

The behavior of harmonics with $n \geq 3$ has not been investigated since the signal strength is much weaker than in second harmonic generation. Moreover, the third harmonic signal only arises from interfaces inside biological tissues.[11] As a consequence, these signals are restricted to very small areas making it difficult to address the laser focus to such a position.

From the theoretical point of view the narrowing factor for the second harmonic should be $\frac{1}{2\sqrt{2}}$ = 0.354 in all measurements. In the calculation, a constant time-bandwidth product of the fundamental and the second harmonic pulse was assumed. This implies, that the pulse characteristics do not change during the process of second harmonic generation. However, slight changes in the time-bandwidth product may have resulted in small deviations between the theoretical predictions and the experimental data (difference between calculated and measured narrowing factors is approximately 0.05).

To sum up, the calculated narrowing factor for the second harmonic wavelength bandwidth is supported by experimental data from non-organic and organic materials. The comparable results of spectral measurements in epi- and trans-direction allow further insight into the phase matching conditions during signal generation. Altogether, these results may help to optimize the spectral separation of signals in multiphoton microscopes.

[1] W. R. Zipfel, R. M. Williams, and W. W. Webb, "Nonlinear magic: multiphoton microscopy in the biosciences," Nature Biotechnology **21**, 1369–1377 (2003).
[2] M. J. Levene, D. A. Dombeck, K. A. Kasischke, R. P. Molloy, and W. W. Webb, "In vivo multiphoton microscopy of deep brain tissue," Journal of Neurophysiology **91**, 1908–1912 (2004).
[3] D. Kobat, M. E. Durst, N. Nishimura, A. W. Wong, C. B. Schaffer, and C. Xu, "Deep tissue multiphoton microscopy using longer wavelength excitation," Optics Express **17**, 13354–13364 (2009).
[4] W. Denk, J. H. Strickler, and W. W. Webb, "Two-photon laser scanning fluorescence microscopy," Science **248**, 73–76 (1990).
[5] W. Denk and K. Svoboda, "Photon upmanship: Why multiphoton imaging is more than a gimmick," Neuron **18**, 351–357 (1997).
[6] F. Helmchen and W. Denk, "Deep tissue two-photon microscopy," Nature Methods **2**, 932–940 (2005).
[7] E. E. Hoover and J. A. Squier, "Advances in multiphoton microscopy technology," Nature Photonics **7**, 93–101 (2013).

[8] X. Chen, O. Nadiarynkh, S. Plotnikov, and P. J. Campagnola, "Second harmonic generation microscopy for quantitative analysis of collagen fibrillar structure," Nature Protocols **7**, 654–669 (2012).
[9] D. Débarre, W. Supatto, and E. Beaurepaire, "Structure sensitivity in third-harmonic generation microscopy," Optics Letters **30**, 2134–2136 (2005).
[10] D. Débarre, W. Supatto, A.-M. Pena, A. Fabre, T. Tordjmann, L. Combettes, M.-C. Schanne-Klein, and E. Beaurepaire, "Imaging lipid bodies in cells and tissues using third-harmonic generation microscopy," Nature Methods **3**, 47–53 (2006).
[11] F. Aptel, N. Olivier, A. Deniset-Besseau, J.-M. Legeais, K. Plamann, M.-C. Schanne-Klein, and E. Beaurepaire, "Multimodal nonlinear imaging of the human cornea," Investigative Ophthalmology & Visual Science **51**, 2459–2465 (2010).
[12] R. W. Boyd, *Nonlinear Optics*, 3rd ed., edited by Boyd (Elsevier Inc., 2008).
[13] G. Latour, I. Gusachenko, L. Kowalczuk, I. Lamarre, and M.-C. Schanne-Klein, "In vivo structural imaging of the cornea by polarization-resolved second harmonic microscopy," Biomedical Optics Express **3**, 1–15 (2011).
[14] P. J. Campagnola, A. C. Millard, M. Terasaki, P. E. Hoppe, C. J. Malone, and W. A. Mohler, "Three-dimensional high-resolution second-harmonic generation imaging of endogenous structural proteins in biological tissues," Biophysical Journal **81**, 493–508 (2002).
[15] W. R. Zipfel, R. M. Williams, R. Christie, A. Y. Nikitin, B. T. Hyman, and W. W. Webb, "Live tissue intrinsic emission microscopy using multiphoton-excited native fluorescence and second harmonic generation," PNAS **100**, 7075–7080 (2003).
[16] W. Mohler, A. C. Millard, and P. J. Campagnola, "Second harmonic generation imaging of endogenous structural proteins," Science Direct - Methods **29**, 97–109 (2003).
[17] J.-C. Diels and W. Rudolph, *Ultrashort Laser Pulse Phenomena: Fundamentals, Techniques and Applications on a Femtosecond Time Scale* (Elsevier Inc., 2006).
[18] G. Wollensak, E. Spoerl, and T. Seiler, "Riboflavin/ultraviolet-a-induced collagen crosslinking for the treatment of keratoconus," American Journal of Ophthalmology **135**, 620–627 (2003).
[19] H. Zhu, T. Wang, W. Zheng, P. Yuan, L. Qian, and D. Fan, "Efficient second harmonic generation of femtosecond laser at 1 μm," Optics Express **12**, 2150–2155 (2004).
[20] J. Zhang, J. Y. Huang, H. Wang, K. S. Wong, and G. K. Wong, "Second-harmonic generation from regeneratively amplified femtosecond laser pulses in BBO and LBO crystals," J. Opt. Soc. Am. B **15**, 200–209 (1998).
[21] J. P. Farrell, L. S. Spector, B. K. McFarland, P. H. Bucksbaum, M. Gühr, M. B. Gaarde, and K. J. Schafer, "Influence of phase matching on the cooper minimum in Ar high-order harmonic spectra," Phys. Rev. A **83**, 023420 (2011).
[22] R. LaComb, O. Nadiarnykh, S. S. Townsend, and P. J. Campagnola, "Phase matching considerations in second harmonic generation from tissues: Effects on emission directionality, conversion efficiency and observed morphology," Optics Communications **281**, 1823–1832 (2008).